Inorganic Chemistry

Article

New Class of Single-Source Precursors for the Synthesis of Main Group−Transition Metal Oxides: Heterobimetallic Pb−Mn β-Diketonates

Haitao Zhang,[†] Jen-Hsien Yang,[†] Roman V. Shpanchenko,[‡] Artem M. Abakumov,[§] Joke Hadermann,[§] Rodolphe Clérac,[||] and Evgeny V. Dikarev*,[†]

[†]*Department of Chemistry, University at Albany, SUNY, Albany, New York, 12222,* [‡]*Department of Chemistry, Lomonosov Moscow State University, Moscow 119991, Russia,* [§]*EMAT, University of Antwerp, Groenenborgerlaan 171, B-2020 Antwerp, Belgium, and* [||]*CNRS, UPR 8641, Centre de Recherche Paul Pascal (CRPP), Equipe "Matériaux Moléculaires Magnétiques", 115 avenue du Dr. Albert Schweitzer, Pessac, F-33600, France and Université de Bordeaux, UPR 8641, Pessac, F-33600, France*

Heterometallic lead−manganese β-diketonates have been isolated in pure form by several synthetic methods that include solid-state and solution techniques. Two compounds with different Pb/Mn ratios, $PbMn_2(hfac)_6$ (**1**) and $PbMn(hfac)_4$ (**2**) (hfac = hexafluoroacetylacetonate), can be obtained in quantitative yield by using different starting materials. Single crystal X-ray investigation revealed that the solid-state structure of **1** contains trinuclear molecules in which lead metal center is sandwiched between two $[Mn(hfac)_3]$ units, while **2** consists of infinite chains of alternating $[Pb(hfac)_2]$ and $[Mn(hfac)_2]$ fragments. The heterometallic structures are held together by strong Lewis acid−base interactions between metal atoms and diketonate ligands acting in chelating-bridging fashion. Spectroscopic investigation confirmed the retention of heterometallic structures in solutions of non-coordinating solvents as well as upon sublimation-deposition procedure. Thermal decomposition of heterometallic diketonates has been systematically investigated in a wide range of temperatures and annealing times. For the first time, it has been shown that thermal decomposition of heterometallic diketonates results in mixed-metal oxides, while both the structure of precursors and the thermolysis conditions have a significant influence on the nature of the resulting oxides. Five different Pb−Mn oxides have been detected by X-ray powder diffraction when studying the decomposition of **1** and **2** in the temperature range 500−800 °C. The phase that has been previously reported as "$Pb_{0.43}MnO_{2.18}$" was synthesized in the pure form by decomposition of **1**, and crystallographically characterized. The orthorhombic unit cell parameters of this oxide, obtained by electron diffraction technique, have been subsequently refined using X-ray powder diffraction data. Besides that, a previously unknown lead−manganese oxide has been obtained at low temperature decomposition and short annealing times. The parameters of its monoclinically distorted unit cell have been determined. The EDX analysis revealed that this compound has a Pb/Mn ratio close to 1:4 and contains no appreciable amount of fluorine.

Introduction

Multimetallic oxides incorporating heavy main group (lead and bismuth) and transition metals are of great interest because of their attractive properties, such as ferro- and piezoelectricity,[1] multiferroism,[2] catalysis,[3] and superconductivity.[4] However, the preparation of lead-containing mixed oxides by traditional high-temperature solid state synthesis is often difficult to control because of the volatility of PbO.[5] It is well-known that some heterometallic coordination complexes with suitable ligands can be used as

*To whom correspondence should be addressed. E-mail: dikarev@albany.edu. Phone: (518)442-4401. Fax: (518)442-3462.

(1) (a) Yoon, K. H.; Kang, D. H. *Encyclopedia of Nanoscience and Nanotechnology*; Nalwa, H. S., Ed.; American Scientific: Stevenson Ranch, 2004; Vol. *8*, pp 435−444. (b) Noheda, B. *Curr. Opin. Solid State Mater. Sci.* **2002**, *6*, 27−34. (c) Ling, H. C.; Yan, M. F. *Mater. Eng.* **1994**, *8*, 397−419. (d) Shirane, G.; Xu, G.; Gehring, P. *Ferroelectrics* **2005**, *321*, 7−19. (e) Noheda, B.; Cox, D. E. *Phase Transitions* **2006**, *79*, 5−20.

(2) (a) Brixel, W.; Rivera, J. P.; Steiner, A.; Schmid, H. *Ferroelectrics* **1988**, *79*, 201−204. (b) Astrov, D. N.; Al'shin, B. I.; Tomashpol'skii, Y. Y.; Venevtsev, Y. N. *Sov. Phys. JETP* **1969**, *28*, 1123. (c) Drobyshev, L. A.; Al'shin, B. I.; Tomashpol'skii, Y. Y.; Venevtsev, Y. N. *Sov. Phys. Crystallogr.* **1969**, *14*, 736−737.

(3) (a) Mullens, C.; Pikulski, M.; Agachan, S.; Gorski, W. *J. Am. Chem. Soc.* **2003**, *125*, 13602−13608. (b) Zhou, W.; Zhao, X.; Wang, Y.; Zhang, J. *Appl. Catal., A* **2004**, *260*, 19−24.

(4) (a) Cava, R. J. *J. Am. Ceram. Soc.* **2000**, *83*, 5−28. (b) Cava, R. J. *Chem. Supercond. Mater.* **1992**, 380−426. (c) Sutherland, M.; Mann, P. D. A.; Bergemann, C.; Yonezawa, S.; Maeno, Y. *Phys. Rev. Lett.* **2006**, *96*, 0970081−0970084. (d) Yonezawa, S.; Maeno, Y. *Phys. Rev. B* **2005**, *72*, 1805041−1805044. (e) Li, M. Y.; Song, Y.; Qu, T. M.; Han, Z. *Physica C* **2005**, *426−431*, 1164−1169.

(5) Daniele, S.; Papiernik, R.; Hubert-Pfalzgraf, L. G.; Jagner, S.; Hakansson, M. *Inorg. Chem.* **1995**, *34*, 628−632.

single-source precursors (SSPs) to obtain crystalline oxide materials upon their decomposition at significantly lower temperatures compared with the solid state or multisource precursor approaches.[6] In addition, the use of SSPs makes it possible to access new phases that are not available at higher reaction temperatures and thus provides more flexibility in the preparation of heterometallic oxide materials than conventional methods.

Despite the fact that many heterometallic lead-transition metal compounds are known,[6–12] only a few of those have been explored as SSPs. The first account appeared in 1994,[8] when a mixture of $PbTiO_3$ and $PbTi_3O_7$ was obtained by decomposition of $Pb_2Ti_4O_2(O_2CCH_3)_2(OC_2H_5)_{14}$. Soon after, Hubert-Pfalzgraf et al. reported[9] a number of Pb−Tr (Tr = Ti, Zr, Nb) alkoxides and studied their decomposition at different temperatures leading to a variety of corresponding tertiary oxides. It was found that the use of SSPs allows one to obtain crystalline oxides at about 100 °C lower than in the process that involves a mixture of homometallic precursors. On the other hand, the thermolysis of lead-rich $Pb_3ZrO(OPr^i)_8$ was shown[10] to yield no heterometallic products. The only reported example of an SSP that does not contain alkoxide ligands[11] is lead−zirconium oxalate, $Pb_2Zr(C_2O_4)_4$, which affords a mixture of $PbZrO_3$ and PbO as decomposition products.

Manganese-based oxides with mixed-valent Mn^{3+}/Mn^{4+} ions have been intensively studied[13] because of their unusual properties, such as charge and orbital ordering, metal/insulator transition, colossal magnetoresistive (CMR) effect,

and magnetic phase separation. The structurally characterized compounds in the Pb−Mn−O system include Pb_2MnO_4,[14,15] $PbMnO_{2.75}$,[16] a hollandite-type mineral of approximate composition $Pb_{1+x}Mn_8O_{16}$,[17] and $Pb_3Mn_7O_{15}$,[15,18] while the identity of several other phases, $Pb_{0.43}MnO_{2.18}$, $Pb_{0.25}MnO_2$, and $Pb_{0.25}MnO_{1.99}$, have been established[15] by their X-ray powder diffraction patterns only. Although, a number of other oxides have also been mentioned in the literature,[16a,17b,19] the careful examination of their X-ray powder diffraction spectra suggests that these compositions are either mixtures of the above-mentioned phases or cation-/oxygen-deficient variations of the latter. All known Pb−Mn oxides were synthesized by conventional solid state reactions, and the application of SSPs for their preparation remains unknown because of the lack of suitable heterometallic Pb−Mn precursor complexes.

Metal β-diketonates have been widely explored as MOCVD precursors for the synthesis of oxide materials.[20] Diketonate complexes exhibit a number of advantages in comparison with other ligands, such as higher volatility, stronger resistance to hydrolysis, and easier structural control of precursors. However, because of their chelating character, β-diketonates are not generally considered as proper ligands for the formation of heterometallic species. Moreover, the rational control of metal stoichiometry in heterometallic complexes is one of the most significant challenges in the synthesis of SSPs. Whitmire has proposed[12] that the formation of Lewis acid−base heterometallic adducts is a viable synthetic approach because of generally high yields, relatively short reaction times, and the absence of complicating side reactions. Recently, we have demonstrated the possibility of utilizing Lewis acid−base interactions for the construction of heterometallic β-diketonates. We suggested several low-temperature solid state synthetic routes that utilize coordinatively unsaturated metal fragments for the formation of bismuth-transition metal[21a] and manganese-containing[21b] heterometallic diketonates. These compounds exhibit high volatility, clean, low-temperature decomposition, and retention of heterometallic structures upon sublimation-deposition as well as in solutions of non-coordinating solvents.

Herein we expand this effective approach to the synthesis of heterometallic lead−manganese diketonates. Compounds with different Pb/Mn ratios (1:2 and 1:1) have been isolated in pure form by several synthetic methods including solid state and solution techniques. For the first time, it has been shown that thermal decomposition of heterometallic diketonates do produce mixed oxides, while both the structure of precursors and thermolysis conditions have a significant

(6) (a) Hubert-Pfalzgraf, L. G. *Inorg. Chem. Commun.* **2003**, *6*, 102–120. (b) Kessler, V. G. *Chem. Commun.* **2003**, 1213–1222. (c) Caulton, K. G.; Hubert-Pfalzgraf, L. G. *Chem. Rev.* **1990**, *90*, 969–995.

(7) (a) Holloway, C. E.; Melnik, M. *Main Group Met. Chem.* **1997**, *20*, 107-132, and references therein. (b) Vigato, P. A.; Tamburini, S. *Coord. Chem. Rev.* **2004**, *248*, 1717-2128, and references therein. (c) Ōkawa, H.; Furutachi, H.; Fenton, D. E. *Coord. Chem. Rev.* **1998**, *174*, 51-75, and references therein. (d) Shiga, T.; Nakanishi, T.; Ohba, M.; Ōkawa, H. *Polyhedron* **2005**, *24*, 2732–2736. (e) Papiernik, R.; Hubert-Pfalzgraf, L. G.; Veith, M.; Huch, V. *Chem. Ber.* **1997**, *130*, 1361–1363. (f) Teff, D. J.; Huffman, J. C.; Caulton, K. G. *Inorg. Chem.* **1996**, *35*, 2981–2987. (g) Teff, D. J.; Huffman, J. C.; Caulton, K. G. *J. Am. Chem. Soc.* **1996**, *118*, 4030−4035, and references therein. (h) Luo, F.; Che, Y. X.; Zheng, J. M. *Inorg. Chem. Commun.* **2006**, *9*, 848–851. (i) Seda, S. H.; Janczak, J.; Lisowski, J. *Inorg. Chem. Commun.* **2006**, *9*, 792–796. (j) Xue, L.; Luo, F.; Che, Y. X.; Zheng, J. M. *J. Mol. Struct.* **2007**, *832*, 132–137. (k) Baidina, I. A.; Krisyuk, V. V.; Stabnikov, P. A. *J. Struct. Chem.* **2006**, *47*, 1111–1116.

(8) Chae, H. K.; Payne, D. A.; Xu, Z.; Ma, L. *Chem. Mater.* **1994**, *6*, 1589–1592.

(9) (a) Daniele, S.; Papiernik, R.; Hubert-Pfalzgraf, L. G.; Jagner, S.; Håkansson, M. *Inorg. Chem.* **1995**, *34*, 628–632. (b) Hubert-Pfalzgraf, L. G.; Daniele, S.; Papiernik, R.; Massiani, M. C.; Septe, B.; Vaissermann, J.; Daran, J. C. *J. Mater. Chem.* **1997**, *7*, 753–762. (c) Boulmaâz, S.; Papiernik, R.; Hubert-Pfalzgraf, L. G.; Septe, B.; Vaissermann, J. *J. Mater. Chem.* **1997**, *7*, 2053–2061. (d) Brethon, A.; Hubert-Pfalzgraf, L. G.; Daran, J. C. *Dalton Trans.* **2006**, 250–257. (e) Brethon, A.; Hubert-Pfalzgraf, L. G. *J. Sol-Gel Sci. Technol.* **2006**, *39*, 159–167, and references therein.

(10) Teff, D. J.; Minear, C. D.; Baxter, D. V.; Caulton, K. G. *Inorg. Chem.* **1998**, *37*, 2547–2553.

(11) Boudaren, C.; Auffrédic, J. P.; Louër, M.; Louër, D. *Chem. Mater.* **2000**, *12*, 2324–2333.

(12) Thurston, J. H.; Tang, C. G. Z.; Trahan, D. W.; Whitmire, K. H. *Inorg. Chem.* **2004**, *43*, 2708–2713.

(13) (a) Adriana, M.; Seiji, Y.; Elbio, D. *Science* **1999**, *283*, 2034–2040, and references therein. (b) Mori, S.; Chen, C. H.; Cheong, S. W. *Nature* **1998**, *392*, 473–476, and references therein.

(14) Teichert, A.; Mueller-Buschbaum, H. *Z. Anorg. Allg. Chem.* **1991**, *598*, 319–325.

(15) Latourrette, B.; Devalette, M.; Guillen, F.; Fouassier, C. *Mater. Res. Bull.* **1978**, *13*, 567–574.

(16) (a) Bougerol, C.; Gorius, M. F.; Grey, I. E. *J. Solid State Chem.* **2002**, *169*, 131–138. (b) Klein, H. *Philos. Mag. Lett.* **2005**, *85*, 569–575.

(17) (a) Post, J. E.; Bish, D. L. *Am. Mineral.* **1989**, *74*, 913–917. (b) Frondel, C.; Heinrich, E. W. *Am. Mineral.* **1942**, *27*, 48–56. (c) Giovanoli, R.; Faller, M. *Chimia* **1989**, *43*, 54–56.

(18) (a) Darriet, B.; Devalette, M.; Latourrette, B. *Acta Crystallogr.* **1978**, *B34*, 3528–3532. (b) Volkov, N. V.; Sablina, K. A.; Bayukov, O. A.; Eremin, E. V.; Petrakovskii, G. A.; Velikanov, D. A.; Balaev, A. D.; Bovina, A. F.; Böni, P.; Clementyev, E. *J. Phys.: Condens. Matter.* **2008**, *20*, 0552171–0552176. (c) Rasch, J. C. E.; Sheptyakov, D. V.; Schefer, J.; Keller, L.; Boehm, M.; Gozzo, F.; Volkov, N. V.; Sablina, K. A.; Petrakovskii, G. A.; Grimmer, H.; Conder, K.; Löffler, J. F. *J. Solid State Chem.* **2009**, *182*, 1188–1192.

(19) Bush, A. A.; Titov, A. V.; Al'shin, B. I.; Venevtsev, Yu. N. *Zh. Neorg. Khim.* **1977**, *22*, 2238–2244.

(20) (a) Hampden-Smith, M. J.; Kodas, T. T.; Ludviksson, A. *Chemistry of Advanced Materials*; Interrante, L. V., Hampden-Smith, M. J., Eds.; Wiley-VCH: New York, 1998; pp 143−206. (b) Doppelt, P. *Coord. Chem. Rev.* **1998**, *178−180*, 1785–1809. (c) Tiitta, M.; Niinisto, L. *Chem. Vap. Deposition* **1997**, *3*, 167–182. (d) Marks, T. J. *Pure Appl. Chem.* **1995**, *67*, 313–318. (e) Spencer, J. T. *Prog. Inorg. Chem.* **1994**, *41*, 145–237.

influence on the nature of the resulting oxides. The phase that has been previously reported[15] as "Pb$_{0.43}$MnO$_{2.18}$" was synthesized in pure form by decomposition of Pb−Mn diketonates and characterized by X-ray powder and electron diffraction (ED) methods. In addition, the existence of a previously unknown lead−manganese oxide was unambiguously confirmed.

Results and Discussion

Synthesis and Properties. In all previous reports on the synthesis of heterometallic β-diketonates,[7k,21] only one M: M′ composition has been obtained in each case. In this work, we demonstrate for the first time that heterometallic diketonates with different Pb/Mn ratios can be isolated by using different starting materials (Scheme 1).

Lead-manganese hexafluoroacetylacetonate, PbMn$_2$-(hfac)$_6$ (**1**), was prepared as sole product of a stoichiometric solid-state redox reaction at 80 °C:

$$Pb + 2Mn(hfac)_3 \rightarrow PbMn_2(hfac)_6 \qquad (1)$$

A complex with 1:1 ratio, PbMn(hfac)$_4$ (**2**), was synthesized in quantitative yield at 100 °C by the solid-state reaction of unsolvated homometallic diketonates:

$$Pb(hfac)_2 + Mn(hfac)_2 \rightarrow PbMn(hfac)_4 \qquad (2)$$
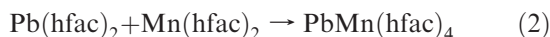
The purity of the products was confirmed by elemental analysis, as well as by X-ray powder diffraction. Importantly, we have shown that reaction (1) can be carried out also in diphenyl ether solution at 100 °C. The latter approach represents the most convenient synthetic route to complex **1** and allows one to obtain it in a pure form on a large scale. In addition, we found that **1** can be stoichiometrically converted to **2** and vice versa by solid state reactions with Pb(hfac)$_2$ and Mn(hfac)$_2$, respectively. Quantitative transformation of **1** to **2** is the preferred method for large scale preparation of the latter. Finally, the reaction between Pb(hfac)$_2$ and Mn metal also affords heterometallic diketonates but as approximately a 50:50 mixture of **1** and **2**. In this reaction, Mn is likely getting oxidized by lead(II) to Mn(hfac)$_2$ which then reacts with an excess of Pb(hfac)$_2$ starting material; however, we cannot exclude the decomposition of the ligand as a source for manganese oxidation.

Heterometallic Pb−Mn β-diketonates revealed different physical properties: complex **1** is soluble in both non-coordinating (dichloromethane, chloroform) and coordinating (acetone, THF) solvents, while **2** is essentially insoluble in non-coordinating solvents. Pale-yellow crystals of **1** loose crystallinity within minutes in open air, while orange-yellow crystals of **2** are relatively stable and can be handled outside the glovebox for a reasonable period of time. Compound **1** is more volatile and can be quantitatively resublimed at 80 °C in a sealed ampule, while **2** needs about 110 °C to be transported. The TGA/DTA data show that the thermal decomposition of compounds **1** and **2** on heating in nitrogen/air proceeds differently and is accompanied by some loss of β-diketonates to sublimation.

Figure 1. Molecular structure of trinuclear heterometallic complex PbMn$_2$(hfac)$_6$ (**1**). Fluorine and hydrogen atoms are omitted for clarity.

Scheme 1
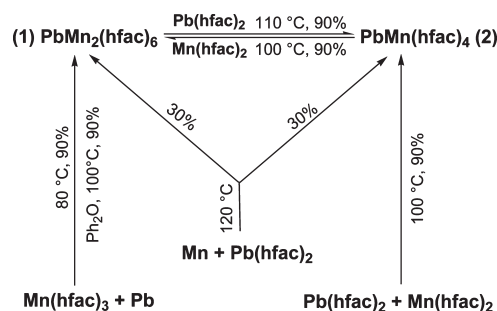
Solid-State and Solution Structures. Single-crystal X-ray analysis revealed that the solid state structure of **1** contains trinuclear molecules in which the lead metal center is sandwiched between two [Mn(hfac)$_3$] groups (Figure 1). All β-diketonate ligands are chelating to manganese atoms, and the heterometallic molecule is held together by six Pb−O contacts (averaged to 2.59 Å) the lengths of which are between the typical chelating and bridging Pb−O distances in diketonate complexes.[7k,22]

The geometry of the manganese atoms in **1** is distorted octahedral with three of the Mn−O bond distances (2.22 Å) being essentially longer than the others (2.13 Å; Table 1) because of the bridging coordination of oxygen atoms in the former to the central Pb atom. The Mn−O distances in **1** are close to those reported for ionic [Mn^{II}(hfac)$_3$]$^-$ species[21b,23] and Mn^{II}(hfac)$_2$L$_2$ adducts (2.12−2.24 Å),[21b,23a,23c] but are significantly longer than the corresponding distances in the homometallic Mn^{III}-(hfac)$_3$ complex (2.00 Å),[23f] indicating that the oxidation state of manganese is +2 in complex **1**. The formula of **1** thus can be written as {Pb^{2+}[Mn(hfac)$_3$]$^-_2$}. This formulation has also been confirmed by magnetic measurements for **1** (vide infra). The trinuclear structure of **1** directly resembles those of the homometallic diketonates [Mn(acac)$_2$]$_3$,[24a] [Mn(hfac)$_2$]$_3$,[23a] [Mg(acac)$_2$]$_3$,[24b] and Ni(*tert*-butyl acetoacetato)$_2$[24c] as well as that of the heterometallic CdMn$_2$(hfac)$_6$[21b] complex.

(21) (a) Dikarev, E. V.; Zhang, H.; Li, B. *J. Am. Chem. Soc.* **2005**, *127*, 6156–6157. (b) Zhang, H.; Li, B.; Dikarev, E. V. *J. Cluster Sci.* **2008**, *19*, 311–321.
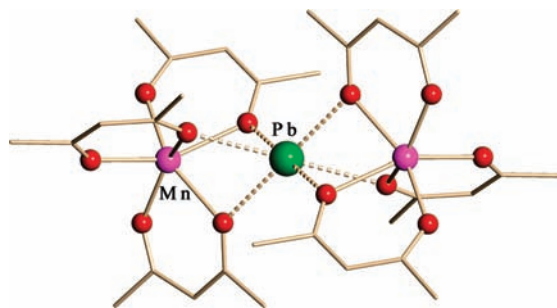
(22) Krisyuk, V. V.; Baidina, I. A.; Igumenov, I. K. *Main Group Met. Chem.* **1998**, *21*, 199–206.

(23) (a) Zhang, H.; Li, B.; Sun, J.; Clérac, R.; Dikarev, E. V. *Inorg. Chem.* **2008**, *47*, 10046–10052. (b) Bryant, J. R.; Taves, J. E.; Mayer, J. M. *Inorg. Chem.* **2002**, *41*, 2769–2776. (c) Troyanov, S. L.; Gorbenko, O. Y.; Bosak, A. A. *Polyhedron* **1999**, *18*, 3505–3509. (d) Parsons, S.; Winpenny, R.; Wood, P. *Private Communication* **2004**. (e) Villamena, F. A.; Dickman, M. H.; Crist, D. R. *Inorg .Chem.* **1998**, *37*, 1446–1453. (f) Bouwman, E.; Caulton, K. G.; Christou, G.; Folting, K.; Gasser, C.; Hendrickson, D. N.; Huffman, J. C.; Lobkovsky, E. B.; Martin, J. D.; Michel, P.; Tsai, H. -L.; Xue, Z. *Inorg. Chem.* **1993**, *32*, 3463–3470.

**Table 1.** Selected M−O Bonding Distances (Å) in Complexes **1** and **2**[a]

	Pb−O$_c$	Pb−O$_{c\text{-}b}$	Pb−O$_b$	Mn−O$_c$	Mn−O$_{c\text{-}b}$	Mn−O$_b$
PbMn$_2$(hfac)$_6$ (**1**)			2.59	2.13	2.22	
PbMn(hfac)$_4$ (**2**)	2.35	2.49, 2.62	2.84, 2.93	2.12	2.20	2.23
	2.38	2.57	2.74, 2.84	2.08	2.10	2.34, 2.81

[a] c − chelating, c-b − chelating-bridging, b − bridging.
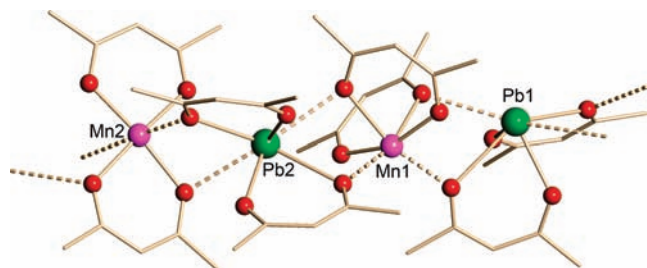
Figure 2. Fragment of the infinite chain structure in heterometallic complex PbMn(hfac)$_4$ (**2**). Fluorine and hydrogen atoms are omitted for clarity.

Heterometallic diketonate PbMn(hfac)$_4$ (**2**) was found to have a polymeric structure in the solid state, which is in accord with its lower volatility and solubility as compared to **1**. The structure consists of infinite zigzag chains of alternating [Mn(hfac)$_2$] and [Pb(hfac)$_2$] units (Figure 2). Each metal center has two chelating β-diketonate ligands, and the oxidation state of each metal atom is thus +2, which is confirmed by magnetic measurements (vide infra). There are four crystallographically independent metal sites (two Mn and two Pb) in the structural motif. The M(hfac)$_2$ (M = Mn, Pb) fragments are connected through Lewis acid−base M−O interactions (2.23−2.81 and 2.74−2.93 Å, Table 1) that are significantly shorter than the sum of the corresponding van der Waals radii (3.52 and 3.54 Å, respectively). Although all metal centers have a coordination number of 6, the coordination environment of each atom is substantially different. Thus, the Mn(1) atom has two chelating β-diketonate groups almost perpendicular to each other (96.3°) and two short bridging Mn−O contacts (2.21 and 2.25 Å) from the neighboring [Pb(hfac)$_2$] units in a *cis*-fashion, while Mn(2) has the two β-diketonates located essentially in a plane (15.3°) with one short (2.34 Å) and one long (2.81 Å) interaction to bridging oxygen atoms in *trans*-positions. Both diketonate ligands chelating the Mn(1) center provide bridging interactions to neighboring Pb atoms, though only one of the diketonates on Mn(2) is involved in interactions with lead.

The solution behavior of Pb−Mn heterometallic β-diketonates was studied by NMR and IR methods. As was already mentioned, only PbMn$_2$(hfac)$_6$ (**1**) is soluble in non-coordinating solvents in accord with its non-polymeric structure. A solution of **1** in CD$_2$Cl$_2$ is NMR silent which supports the idea that the manganese atoms have a d^5 high-spin electronic configuration. It also indicates the retention of the trinuclear structure of **1** in non-coordinating solvents. On the contrary, in coordinating solvents such as d_6-acetone, singlets for proton (δ = 5.80 ppm) and fluorine (δ = −76.40 ppm) atoms immediately appear in the NMR spectra of **1**. These signals were confirmed as belonging to the acetone adduct of Pb(hfac)$_2$. In addition, a *trans*-Mn(hfac)$_2$(Me$_2$CO)$_2$[23a]
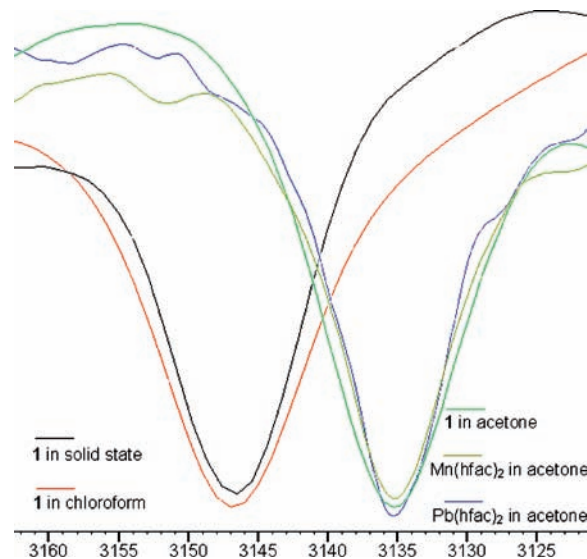
Figure 3. Infrared C−H stretching frequencies for hetero- and homo-metallic diketonates.

complex (NMR silent) can be instantly crystallized from an acetone solution of **1**. The NMR spectra of **2**, which is soluble in coordinating solvents only, reveal similar peaks (5.81 and −76.38 ppm, respectively for ^{1}H and ^{19}F). All these observations point to the disruption of the heterometallic structure and the formation of homometallic solvates in coordinating solvents.

The IR study of **1** shows the same C−H stretching positions for the solid state and chloroform solution, while in acetone solution, the C−H peak down shifts about 10 cm^{-1} (Figure 3). The latter C−H frequency is the same for acetone solutions of homometallic diketonates, Pb(hfac)$_2$ and Mn(hfac)$_2$. The difference is related to the change in coordination mode of the β-diketonate ligands from chelating-bridging to pure chelating, as we have shown previously.[21b,23a] These data also indicate the retention of heterometallic structure **1** in non-coordinating solvents as well as its collapse, accompanied by chelating diketonate ligands redistribution, in the presence of strong donor molecules.

Magnetic Susceptibility Studies for Heterometallic Pb−Mn Diketonates. At room temperature, the χT products for **1** (8.7 cm$^3 \cdot$K/mol) and **2** (4.3 cm$^3 \cdot$K/mol) are in good agreement with the presence of two and one, respectively, S = 5/2 Mn^{II} metal ions (for each S = 5/2 Mn^{II} metal ion: C = 4.375 cm$^3 \cdot$K/mol expected for g = 2) and with the theoretical values of 8.75 (**1**) and 4.375 (**2**) cm$^3 \cdot$K/mol. These results confirm the assignment of the manganese oxidation states based on the structural data (vide supra). Upon decreasing the temperature, the χT products at 1000 Oe are almost constant and only slightly decrease below 8 K to reach 7.80 (**1**) and 3.71 (**2**) cm$^3 \cdot$K/mol at 1.8 K (Figure 4) indicating dominant but very weak
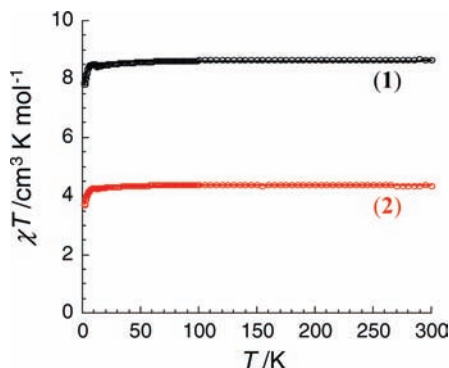
Figure 4. χT vs T plots for **1** and **2** at 1000 Oe (χ being the magnetic susceptibility equal to M/H normalized by trinuclear complex and chain repeating unit, respectively). The solid lines are the best fits of the experimental data with the Curie−Weiss law as described in the text.

antiferromagnetic interactions within the trinuclear $PbMn_2(hfac)_6$ complex and $[PbMn(hfac)_4]_\infty$ chains.

Fit of the thermal behavior with a Curie−Weiss law leads to $C = 8.6$ (**1**), 4.36 (**2**) $cm^3 \cdot K/mol$ and $\theta = -0.2$ K. It is worth noting that the Curie constants are in very good agreement with the theoretical values quoted above. Moreover, the negative sign of the Weiss constant confirms the presence of dominant antiferromagnetic interactions. Heisenberg $S = 5/2$ dimer model ($H = -2J \{S_{Mn(1)} \bullet S_{Mn(2)}\}$) for compound **1** and $S = 5/2$ chain model ($H = -2J \Sigma S_{Mn(i)} \bullet S_{Mn(i+1)}$) for compound **2** lead also to very good fits of the data with $J/k_B = -0.03$ K and $g = 1.99$ in both cases. On the basis of these considerations, the magnetic interactions between Mn^{II} metal ions through both the $[O_3PbO_3]$ bridge in **1** and the $[O_2PbO_2]$ bridge in **2** are very weak.

Thermal Decomposition. The primary goal of this research was to test the application of heterometallic diketonates as SSPs for the synthesis of oxide materials. The two lead−manganese diketonates, $PbMn_2(hfac)_6$ (**1**) and $PbMn(hfac)_4$ (**2**), offer a unique opportunity to study the influence of the metal ratio and precursor structure on the identity of decomposition products. The analysis of thermolysis traces confirmed that *heterometallic diketonates do produce mixed oxides upon their decomposition/annealing.* Four different known Pb−Mn oxides have been detected by X-ray powder diffraction when studying the decomposition of **1** and **2** in the temperature range 500−800 °C. Table 2 shows the major phases present in the decomposed samples; most of the products also contain small amounts of different binary and ternary oxides.

Decomposition of **1** at 500 °C results (Figure 5A) in a mixture of lead(IV) fluoride, $Pb_{1+x}Mn_8O_{16}$[17a] oxide and at least two new phases (*A* and *B*) that have not been identified before. Increasing the decomposition temperature to 600 °C leads to the complete disappearance of PbF_4 and one of the new phases (*B*). The amount of remaining new phase (*A*) drastically decreases with an elongation of the annealing time. The phase identified before[15] as "$Pb_{0.43}MnO_{2.18}$" appears at 600 °C and becomes the major component, whereas $Pb_{1+x}Mn_8O_{16}$ disappears, if the annealing continues for more than 24 h. "$Pb_{0.43}MnO_{2.18}$" is present in an almost pure form in the powder X-ray diffraction spectrum of the sample that was annealed at 600 °C for 3 days. When the decomposition

temperature was increased to 700 °C, the product became a mixture of "$Pb_{0.43}MnO_{2.18}$" and $Pb_3Mn_7O_{15}$.[15,18] It was found that further increase of the temperature favored the formation of $Pb_3Mn_7O_{15}$, which was the only product of decomposition at 800 °C (Figure 5C).

The decomposition of **2** at 500 °C (72 h) produces a mixture of Pb_2MnO_4[14,15] and $Pb_{1+x}Mn_8O_{16}$ oxides with unknown crystalline phases *A* and *B*; the latter likely contains some fluorine. At 600 °C all these phases effectively disappear, except *A* that is present as a mixture with lead(II) oxide. However, after 3 days of annealing at 600 °C the analysis indicates a mixture of Pb_2MnO_4 and "$Pb_{0.43}MnO_{2.18}$" (Figure 5B). At higher temperatures (800 °C), the thermolysis of **2** gives the same product, $Pb_3Mn_7O_{15}$, as **1** under the same conditions.

It is worth stressing that the Pb/Mn ratio in heterometallic diketonates influences the nature of their decomposition products. While decomposition of **1** and **2** is clearly different at low temperatures, it produces similar results when the temperature is increased. At 500 °C there is still some amount of fluorine remaining; however, at higher temperatures, there was no fluorine residue in the products detected by elemental analysis. The decomposition process for both diketonates at low temperatures/ short annealing times results in multiphasic mixtures. Apparently, equilibrium is not achieved in these cases, and the phase composition keeps changing as the annealing time is increased. At 600 °C, the Pb/Mn ratio in the resulting oxides corresponds well with the metal ratio in the precursors. On the other hand, at 800 °C the Pb/Mn = 3:7 ratio for both compounds can be explained by the mass loss because of the volatility of PbO that occurs above 700 °C.[25]

Crystallographic Characterization of the Pb−Mn Oxides. The results of thermal decomposition allowed us to crystallographically characterize the "$Pb_{0.43}MnO_{2.18}$" compound and the new phase *A*. The lattice parameters and space symmetry for "$Pb_{0.43}MnO_{2.18}$" were investigated using ED. The representative [010] and [100] ED patterns (Figure 6) demonstrate a high degree of crystallinity for the "$Pb_{0.43}MnO_{2.18}$" compound. The orthorhombic lattice parameters found by examining a set of reciprocal space sections were subsequently refined using X-ray powder diffraction data as $a = 13.8392(6)$, $b = 11.2198(5)$, $c = 9.9437(4)$ Å, $V = 1544.0(2)$ Å^3. The extinction conditions found on the ED and X-ray powder diffraction data are in agreement with the most symmetric space group $Pnma$. It should be noted that forbidden $h00$, $h \neq 2n$ and $00l$, $l \neq 2n$ reflections on the [010] ED pattern are caused by multiple diffraction that was confirmed by observation of the intensity of the forbidden reflections upon tilting the crystal along the corresponding reciprocal lattice axes, as well as by the absence of the $00l$, $l \neq 2n$ reflections on the [100] ED pattern.

Indexing of the X-ray powder diffraction pattern revealed that the sample annealed at 600 °C for 72 h represents an essentially pure "$Pb_{0.43}MnO_{2.18}$" phase

(24) (a) Shibata, S.; Onuma, S.; Inoue, H. *Inorg. Chem.* **1985**, *24*, 1723–1725. (b) Weiss, E.; Kopf, J.; Gardein, T.; Corbelin, S.; Schumann, U. *Chem. Ber.* **1985**, *118*, 3529–3534. (c) Dohring, A.; Goddard, R.; Jolly, P. W.; Kruger, C.; Polyakov, V. R. *Inorg. Chem.* **1997**, *36*, 177–183.
(25) Chen, Z.; Zeng, Y.; Yang, C.; Yang, B. *Mater. Sci. Eng., B* **2005**, *123*, 143–148.

Table 2. Results of Thermal Decomposition of Heterometallic Diketonates at Different Temperatures and Annealing Times[a]

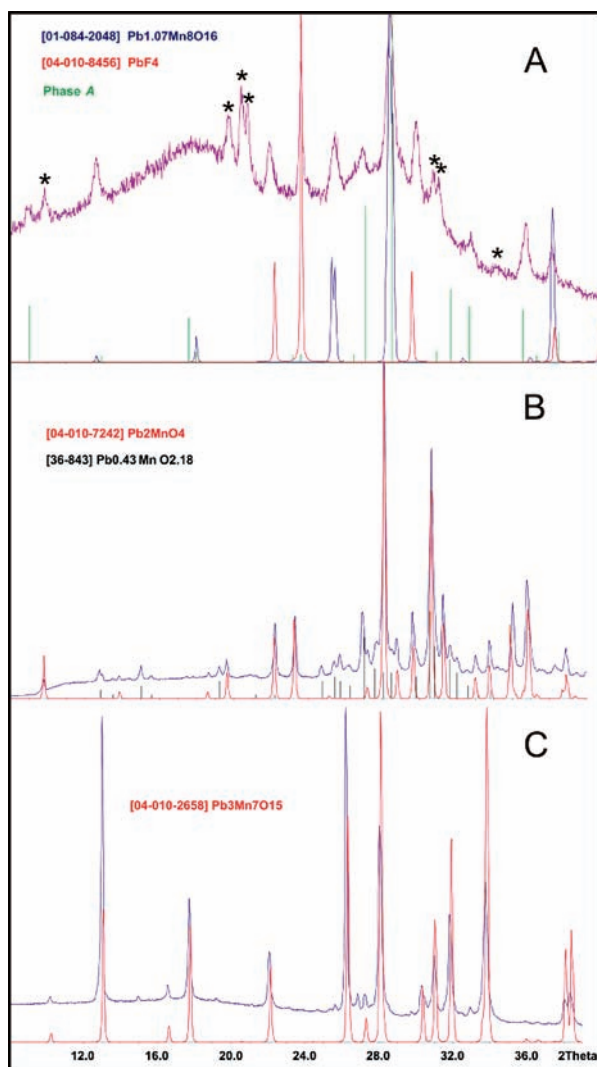| temp/time	$PbMn_2(hfac)_6$ (**1**)	$PbMn(hfac)_4$ (**2**)
500 °C/72 h	$Pb_{1+x}Mn_8O_{16} + PbF_4 + A + B$	$Pb_2MnO_4 + Pb_{1+x}Mn_8O_{16} + A + B$
600 °C/0.5 h	$Pb_{1+x}Mn_8O_{16} + PbO + A$	$PbO + A$
600 °C/3 h	$Pb_{1+x}Mn_8O_{16} + Pb_{0.43}MnO_{2.18} + A$	
600 °C/24 h	$Pb_{1+x}Mn_8O_{16} + Pb_{0.43}MnO_{2.18}$	
600 °C/72 h	$Pb_{0.43}MnO_{2.18}$	$Pb_2MnO_4 + Pb_{0.43}MnO_{2.18}$
700 °C/72 h	$Pb_{0.43}MnO_{2.18} + Pb_3Mn_7O_{15}$	
800 °C/72 h	$Pb_3Mn_7O_{15}$	$Pb_3Mn_7O_{15}$

[a] A, B − unknown phases.

Figure 5. Phase identification in oxide samples obtained by decomposition: (A) **1** at 500 °C/72 h; (B) **2** at 600 °C/72 h; (C) **1** at 800 °C/72 h. Peaks corresponding to phase B are marked with asterisk. Phase A is shown as a peak diagram.

(Figure 7). It should be noted that many diffraction peaks that belong to "$Pb_{0.43}MnO_{2.18}$" were not included in the PDF2 standard pattern #00−036−0843 for this compound.

The ED patterns of phase A are shown in Figure 8. The sharp reflections were indexed using the pseudotetragonal unit cell with parameters $a \approx b \approx 14.0$, $c \approx 2.89$ Å. Diffuse satellites, also visible on the ED patterns, can be indexed with $\mathbf{q} \approx 0.74\mathbf{c}^*$. Tilting the crystals around the [001] reciprocal lattice axis revealed that streaks passing
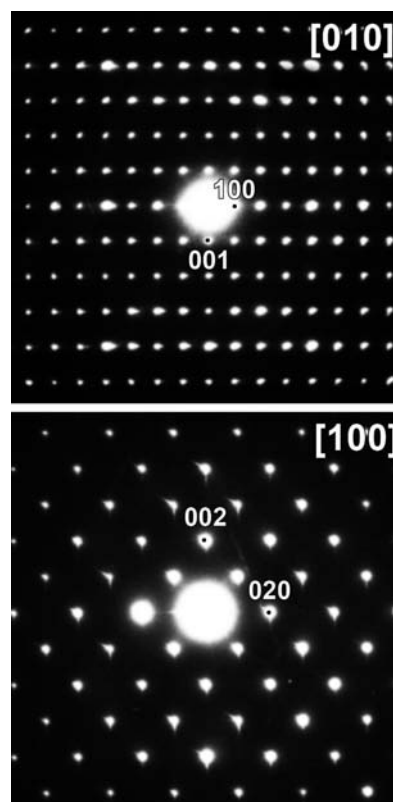

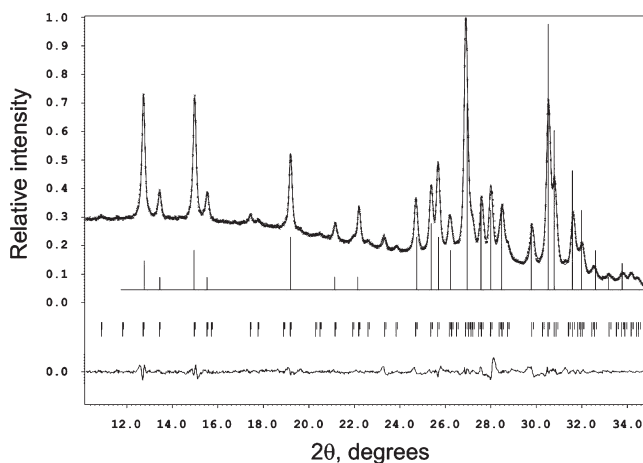**Figure 6.** ED patterns of "$Pb_{0.43}MnO_{2.18}$".

Figure 7. Le Bail fitting for X-ray powder pattern of "$Pb_{0.43}MnO_{2.18}$". Theoretical peak positions are shown at the bottom. Upper peaks correspond to the PDF2 card #00−036−0843.

through the satellite reflections are the traces of diffuse intensity sheets perpendicular to $\mathbf{c}^*$. Best indexing of the
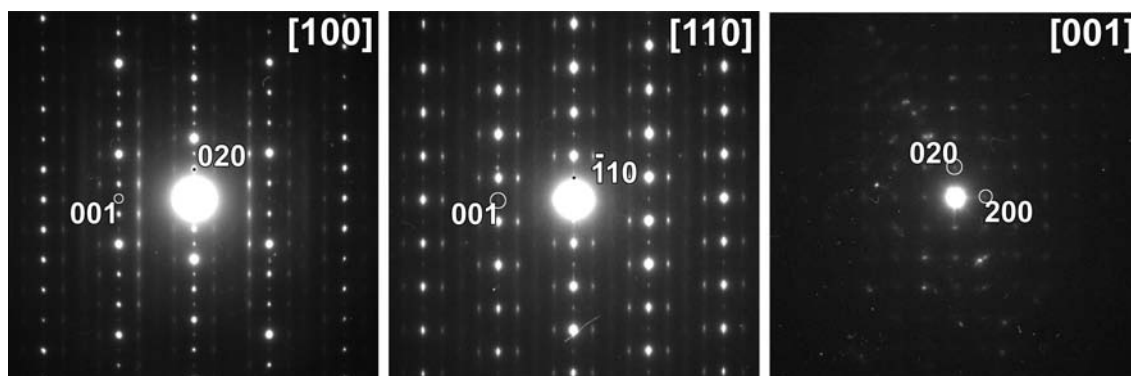
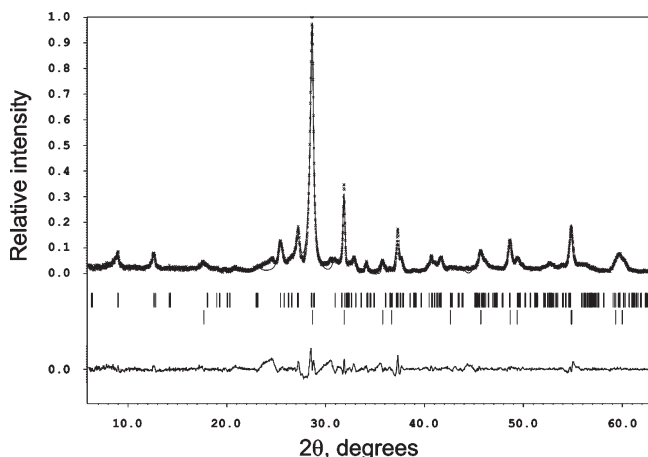**Figure 8.** ED patterns of the phase *A*. The indexing is performed in the pseudotetragonal unit cell.

Figure 9. Le Bail fitting for X-ray powder pattern of phase *A*. The fit was performed for basic unit cell of phase *A*, without taking satellites into account. The bottom row marks correspond to positions of the PbO reflections.

X-ray powder diffraction pattern of phase *A* (Figure 9) was achieved in a monoclinically distorted unit cell with the parameters $a = 14.004(2)$, $b = 13.802(2)$, $c = 2.8865(3)$ Å, $\gamma = 90.14(3)°$. The EDX analysis indicates that the Pb/Mn atomic ratio in the phase *A* is 0.24(4) with no detectable amount of fluorine. At the same time, its powder pattern does not correspond to any of the lead-manganese oxides, including those $Pb_{0.25}MnO_2$ and $Pb_{0.25}MnO_{1.99}$ that have been reported earlier.[15]

Complete characterization of the chemical compositions and crystal structures of the "$Pb_{0.43}MnO_{2.18}$" and *A* phases will be published separately.[26]

Conclusions

In this work we demonstrated that strong Lewis acid-base interactions offer a convenient and direct route to the synthesis of heterometallic β-diketonates. The use of different starting materials and reaction conditions allows one to obtain compounds with different Pb/Mn ratios. The proposed reactions are high-yield processes that can be performed on a large scale. For the first time, it was shown that heterometallic β-diketonates can be utilized as SSPs for the synthesis of complex oxides. It was found that the composi-

tion and structure of precursors, as well as the thermolysis/annealing conditions, have a profound influence on the resulting oxide products. Decomposition of Pb-Mn heterometallic diketonates at different temperatures and annealing times affords a variety of Pb-Mn oxides, including some that have not been previously reported. We believe that the most interesting results can be obtained by studying the decomposition of heterometallic diketonates at low temperatures (≤ 500 °C) and short annealing times. Such investigations that may provide access to yet unknown oxides/oxofluorides are currently underway.

Experimental Section

General Procedures. All of the manipulations were carried out in a dry, oxygen-free, dinitrogen atmosphere by employing standard Schlenk line and glovebox techniques. $Pb(hfac)_2$ was purchased from Strem and purified by recrystallization from $CHCl_3$ solution; lead was purchased from Strem and used as received; manganese, manganese(III) oxide, and hexafluoroacetylacetone were purchased from Aldrich and used as received; diphenyl ether was purchased from Acros Organics and purified as reported.[27] $Mn(hfac)_3$ and $Mn(hfac)_2$ were prepared according to the literature procedures.[23a] UV-vis spectra were acquired using a Hewlett-Packard 8452A diode array spectrophotometer. The attenuated total reflection (ATR) and solution IR spectra were recorded on a PerkinElmer Spectrum 100 FT-IR spectrometer. NMR spectra were obtained using a Bruker Avance 400 spectrometer at 400 MHz for ^1H and at 376.47 MHz for ^{19}F. Chemical shifts (δ) are given in ppm relative to residual solvent peak for ^1H and to $CFCl_3$ for ^{19}F. Elemental analysis was performed by Maxima Laboratories Inc., Ontario, Canada. Thermogravimetric measurements were carried out under nitrogen or air at a heating rate of 5 °C/min using a TGA 2050 thermogravimetric analyzer, TA Instruments, Inc. The thermal decomposition/annealing of heterometallic complexes was studied in air at ambient pressure. The solid samples were placed into a 20 mL Coors high-alumina crucible (Aldrich) and heated at a rate of about 20 °C/min in a 120 V muffle furnace (Thermolyne). The decomposition residues were cooled by turning off the furnace power.

Synthesis. $PbMn_2(hfac)_6$ (1). Method 1. A mixture of Mn-$(hfac)_3$ (0.20 g, 0.30 mmol) and lead granules (0.06 g, 0.30 mmol) was sealed in an evacuated glass ampule and placed in an electric furnace having a temperature gradient along the length of the tube. The ampule was kept at 80 °C for 3 days to allow pale yellow cubic-shaped crystals to be deposited in the cold section of the container where the temperature was set approximately 5 °C lower. Yield is about 90% (crystals collected). The purity of

(26) Abakumov, A. M.; Hadermann, J.; Tsirlin, A. A.; Tan, H.; Verbeeck, J.; Zhang, H.; Dikarev, E. V.; Shpanchenko, R. V.; Antipov, E. V. *J. Solid State Chem.* **2009**, *182*, DOI: 10.1016/j.jssc.2009.06.003.

(27) Perrin, D. D.; Armarego, W. L. F.; Perrin, D. R. *Purification of Laboratory Chemicals*, 2nd ed.; Pergamon Press: Oxford, U.K., 1980; p 383.

the bulk product has been confirmed by comparison of the powder diffraction pattern with the theoretical one calculated on the basis of single crystal data analysis.

Method 2. A mixture of $PbMn(hfac)_4$ (**2**) (0.20 g, 0.18 mmol) and $Mn(hfac)_2$ (0.09 g, 0.20 mmol) was sealed in an evacuated glass ampule and placed in an electric furnace. The ampule was kept at 100 °C for 2 days to allow pale yellow crystals to be deposited in the cold section of the container. Yield is about 90% (crystals collected).

Method 3. A mixture of $Mn(hfac)_3$ (0.40 g, 0.59 mmol) and Pb metal (0.20 g, 0.97 mmol) in 15 mL of diphenyl ether was refluxed at 100 °C for 12 h. The hot solution was transferred to another flask by cannula to separate from the excess of Pb and was kept at room temperature for 8 h to allow precipitation and crystal growth. Diphenyl ether was then removed by cannula, and the yellow precipitate was washed three times with hexanes and dried under vacuum. Yield is about 90%. Elemental analysis (%) calcd for $C_{30}H_6O_{12}F_{36}Mn_2Pb$: C, 23.09; H, 0.38; O, 12.32; F, 43.87; Mn, 7.06; Pb, 13.28; found: C, 23.44; H, 0.32; O, 12.04; F, 44.24; Mn, 6.73; Pb, 12.83. ^1H NMR (d_6-acetone, 22 °C): δ = 5.80 (s); ^{19}F NMR (d_6-acetone, 22 °C): δ = −76.40 (s). ATR−IR (cm^{-1}): 3146w, 1646s, 1616w, 1564m, 1538s, 1463s, 1345w, 1257s, 1215s, 1148s, 1089w. IR ($CHCl_3$, cm^{-1}): 3147w, 1646s, 1615w, 1565m, 1537s, 1460s, 1346w, 1251s, 1215s, 1152s, 1093w. UV/vis (CH_2Cl_2, 22 °C): λ_{max} (ε, $M^{-1} \cdot cm^{-1}$) = 242 (887), 310 (2731) nm.

$PbMn(hfac)_4$ (2). **Method 1.** A mixture of $Mn(hfac)_2$ (0.08 g, 0.17 mmol) and $Pb(hfac)_2$ (0.25 g, 0.40 mmol) was sealed in an evacuated glass ampule and placed in an electric furnace. The ampule was kept at 100 °C for 2 days to allow orange-yellow prismatic crystals to be deposited in the cold section of the container where the temperature was set approximately 5 °C lower. Yield is about 90% (crystals collected). The purity of the bulk product has been confirmed by comparison of the powder diffraction pattern with the theoretical one calculated on the basis of single crystal data analysis.

Method 2. A mixture of $Pb(hfac)_2$ (0.20 g, 0.32 mmol) and manganese powder (10 mg, 0.18 mmol) was sealed in an evacuated glass ampule and placed in an electric furnace. The ampule was kept at 120 °C for 3 days to allow orange-yellow crystals of **2** (ca. 30% based on the initial amount of lead) to be deposited in the cold section of the container along with pale yellow crystals of **1** (ca. 30%). The presence of two compounds was confirmed and the ratio of **1**:**2** was estimated by recording a powder diffraction pattern of the bulk product.

Method 3. A mixture of $PbMn_2(hfac)_6$ (**1**) (0.20 g, 0.13 mmol) and $Pb(hfac)_2$ (0.10 g, 0.15 mmol) was sealed in an evacuated glass ampule and placed in an electric furnace. The ampule was kept at 110 °C for 2 days to allow orange-yellow crystals to be deposited in the cold section of the container. Yield is about 90% (crystals collected). Elemental analysis (%) calcd for $C_{20}H_4O_8F_{24}MnPb$: C, 22.02; H, 0.37; O, 11.74; F, 41.83; Mn, 5.05; Pb, 18.99; found: C, 22.37; H, 0.50; O, 12.13; F, 40.97; Mn, 4.81; Pb, 18.92. ^1H NMR (d_6-acetone, 22 °C): δ = 5.81 (s); ^{19}F NMR (d_6-acetone, 22 °C): δ = −76.38 (s). ATR−IR (cm^{-1}): 3146w, 1648s, 1616w, 1564m, 1538s, 1464s, 1345w, 1258s, 1215s, 1148s, 1092w. UV/vis (CH_2Cl_2, 22 °C): λ_{max} (ε, $M^{-1} \cdot cm^{-1}$) = 242(802), 302(1507) nm.

Magnetic Measurements. The magnetic susceptibility measurements for **1** and **2** were obtained with the use of a Quantum Design SQUID magnetometer MPMS-XL. This magnetometer works between 1.8 and 400 K for direct current (dc) applied fields ranging from −7 to 7 T. Measurements were performed on finely ground crystalline samples (48.8 and 32.8 mg, respectively) prepared in a glovebox under argon and sealed in a plastic bag to avoid any contact with air or water. The presence of ferromagnetic impurities was checked by measuring the magnetization as a function of the field at 100 K. A perfect linear field dependence of the magnetization was found

Table 3. Crystallographic Data and Structure Refinement Parameters

	1	2
formula	$PbMn_2O_{12}C_{30}H_6F_{36}$	$PbMnO_8C_{20}H_4F_{24}$
fw	1559.42	1090.36
crystal system	triclinic	monoclinic
space group	$P\bar{1}$	$P2_1/c$
a (Å)	9.5223(19)	14.517(3)
b (Å)	12.124(2)	21.566(4)
c (Å)	12.224(2)	19.831(4)
α (deg)	117.96(3)	90.00
β (deg)	97.64(3)	91.58(3)
γ (deg)	107.01(3)	90.00
V (Å^3)	1129.4(4)	6206(2)
Z	1	8
ρ_{calcd} (g·cm^{-3})	2.293	2.334
μ (mm^{-1})	4.474	6.013
transm factors	0.5534−0.8413	0.1255−0.5323
temp (K)	173(2)	173(2)
data/restr/params	5038/60/391	14591/174/1047
$R1$,^{a}$wR2^b$		
$I > 2\sigma(I)$	0.043, 0.098	0.040, 0.103
all data	0.049, 0.101	0.048, 0.108
quality-of-fit^c	1.043	1.046

$^a R1 = \sum ||F_o| - |F_c||/\sum |F_o|$. $^b wR2 = [\sum w(F_o^2 - F_c^2)^2/\sum w(F_o^2)^2]^{1/2}$. ^{c} Quality-of-fit $= [\sum [w(F_o^2 - F_c^2)^2]/(N_{obs} - N_{params})]^{1/2}$, based on all data.

indicating the absence of any ferromagnetic impurities. The alternating current (ac) susceptibility was measured with an oscillating ac field of 3 Oe, and ac frequencies ranging from 1 to 1500 Hz, with no out-of-phase ac signal, have been detected above 1.8 K. The magnetic data were corrected for the sample holder and the diamagnetic contribution.

Electron Diffraction. The samples for the electron microscopy investigation were prepared by crushing the powder sample in ethanol and depositing it on a holey carbon grid. ED studies were performed using a Philips CM20 microscope.

X-ray Diffraction Procedures. X-ray powder diffraction data were collected on an automated STADI-P (STOE) diffractometer (Cu K$_{\alpha 1}$ radiation, λ = 1.5406 Å, Ge-monochromator, linear-PSD) in transmission mode with a step of 0.01° 2θ at 20 °C and on a Bruker D8 Advance diffractometer (Cu K$_\alpha$ radiation, focusing Göbel Mirror, LynxEye one-dimensional detector, step of 0.02° 2θ, 20 °C). The crystalline samples under investigation were ground and placed in the dome-like airtight zero-background holders inside a glovebox. The JANA2000 program package[28] was used for the treatment of the X-ray powder diffraction patterns.

Selected single crystals of **1** and **2** suitable for X-ray crystallographic analysis were used for structural determination. The X-ray intensity data were measured at 173(2) K (Bruker KRYOFLEX) on a Bruker SMART APEX CCD-based X-ray diffractometer system equipped with a Mo-target X-ray tube (λ = 0.71073 Å) operated at 1800 W power. The data collection and refinement procedures have been described elsewhere.[21b] The hydrogen atoms were included in idealized positions for structure factor calculations. The fluorine atoms of some CF_3 groups appeared to be disordered over two or three rotational orientations. Anisotropic displacement parameters were assigned to all non-hydrogen atoms, except the disordered fluorines. Relevant crystallographic data are summarized in Table 3.

(28) Petricek, V.; Dusek, M. *JANA2000: Programs for Modulated and Composite Crystals*; Institute of Physics: Praha, Czech Republic, 2000.

Supporting Information Available: Synthetic details for Mn-(hfac)$_2$ and Mn(hfac)$_3$, TGA traces of thermal decomposition for **1** and **2**, ^{1}H and ^{19}F NMR spectra of **1** and **2** in d_6-acetone, X-ray powder patterns for the bulk products in the synthesis of **1** and **2**, additional details on interatomic distances and angles in the structures of **1** and **2**, X-ray crystallographic files for **1** and **2** in CIF format. This material is available free of charge via the Internet at http://pubs.acs.org.